Displacement Assay for the Detection of Stabilizers of Inactive Kinase Conformations[†]

Sabine Klüter,[‡] Christian Grütter,[‡] Tabassum Naqvi,[§] Matthias Rabiller,[‡] Jeffrey R. Simard,[‡] Vijaykumar Pawar,[‡] Matthäus Getlik,[‡] and Daniel Rauh*,[‡]

[‡]*Chemical Genomics Centre of the Max Planck Society, Otto-Hahn-Strasse 15, D-44227 Dortmund, Germany and*
[§]*DiscoveRx Corporation, 42501 Albrae Street, Fremont, California 94538*

Received August 30, 2009

Targeting protein kinases with small molecules outside the highly conserved ATP pocket to stabilize inactive kinase conformations is becoming a more desirable approach in kinase inhibitor research, since these molecules have advanced pharmacological properties compared to compounds exclusively targeting the ATP pocket. Traditional screening approaches for kinase inhibitors are often based on enzyme activity, but they may miss inhibitors that stabilize inactive kinase conformations by enriching the active state of the kinase. Here we present the development of a kinase binding assay employing a pyrazolourea type III inhibitor and enzyme fragment complementation (EFC) technology that is suitable to screen stabilizers of enzymatically inactive kinases. To validate this assay system, we report the binding characteristics of a series of kinase inhibitors to inactive p38α and JNK2. Additionally, we present protein X-ray crystallography studies to examine the binding modes of potent quinoline-based DFG-out binders in p38α.

Introduction

Protein kinases serve as major factors in regulating cell signaling pathways, since they are responsible for the transfer of the γ-phosphate from ATP to various substrate proteins, thereby modulating their function. Kinase disregulation can contribute to diseases such as cancer, Alzheimer's disease, diabetes, and chronic inflammation.[1−5] Over the past two decades, protein kinases have become one of the major classes of targets for drug discovery, resulting in the development of multiple clinically approved kinase inhibitors.[5,6] However, limited selectivity of ATP-competitive (type I) inhibitors has increasingly hampered drug development, particularly for treatment of chronic diseases. Type I inhibitors bind to the active state (DFG-in) of the kinase and have to compete with high cellular concentrations of ATP. Additionally, the high conservation of amino acids lining the ATP binding site among all kinases makes the development of selective small molecules particularly challenging. These impediments have led to increased interest in identifying inhibitors with alternative binding modes that exploit the conformational variability of protein kinases.[7] A major conformational change undergone by many protein kinases is the switch between the active DFG-in and inactive DFG-out conformation, during which the rearrangement of the activation loop opens up a hydrophobic pocket adjacent to the catalytic site.[8] This allosteric pocket can be targeted by type III inhibitors which stabilize the DFG-out state and prevent the kinase domain from adopting the enzymatically competent DFG-in conformation. Type II inhibitors such as imatinib and sorafenib (**25**)[9] also occupy this site but, in addition, extend into the ATP binding region of the catalytic cleft to form additional interactions with the hinge region of the kinase domain.[10] Type II/III inhibitors not only are perceived to have superior selectivity profiles but also, because of their slow off-rates and increased drug-target residence times, have advanced pharmacological properties.[10] Despite the advantages of such ligands, methods for identifying type II/III inhibitors are limited and most are unsuitable for high-throughput screening (HTS) initiatives. Additionally, there is no simple method available at all to predict whether a kinase of interest can even adopt the DFG-out conformation.

Existing kinase screening methods are mainly based on enzyme activity assays.[11,12] Since active kinases are typically in the DFG-in conformation, these assays create a bias for the identification of classic type I inhibitors and, therefore, may not be particularly suitable for detecting the lower affinity type III inhibitors which have proven to be valuable starting points for the development of more potent type II inhibitors.[10,13] To circumvent the difficulties associated with the use of activity assays for the discovery of DFG-out binders, we set out to develop a kinase binding assay using a type III inhibitor probe combined with an enzyme fragment complementation technology (Figure 1a).[14,15] The assay makes use of a labeled probe consisting of a type III inhibitor chemically conjugated to a small (∼5 kDa) enzyme donor (ED[a]) peptide fragment of β-galactosidase. This conjugated enzyme fragment complements an inactive fragment of β-galactosidase (enzyme acceptor or EA), forming an active enzyme that generates a

---

[a]Abbreviations: ED, enzyme donor; EFC, enzyme fragment complementation; FRET, fluorescence resonance energy transfer; FLiK, fluorescent labels in kinases; K_d, dissociation constant; JNK2, c-Jun N-terminal kinase 2; cpd, compound.
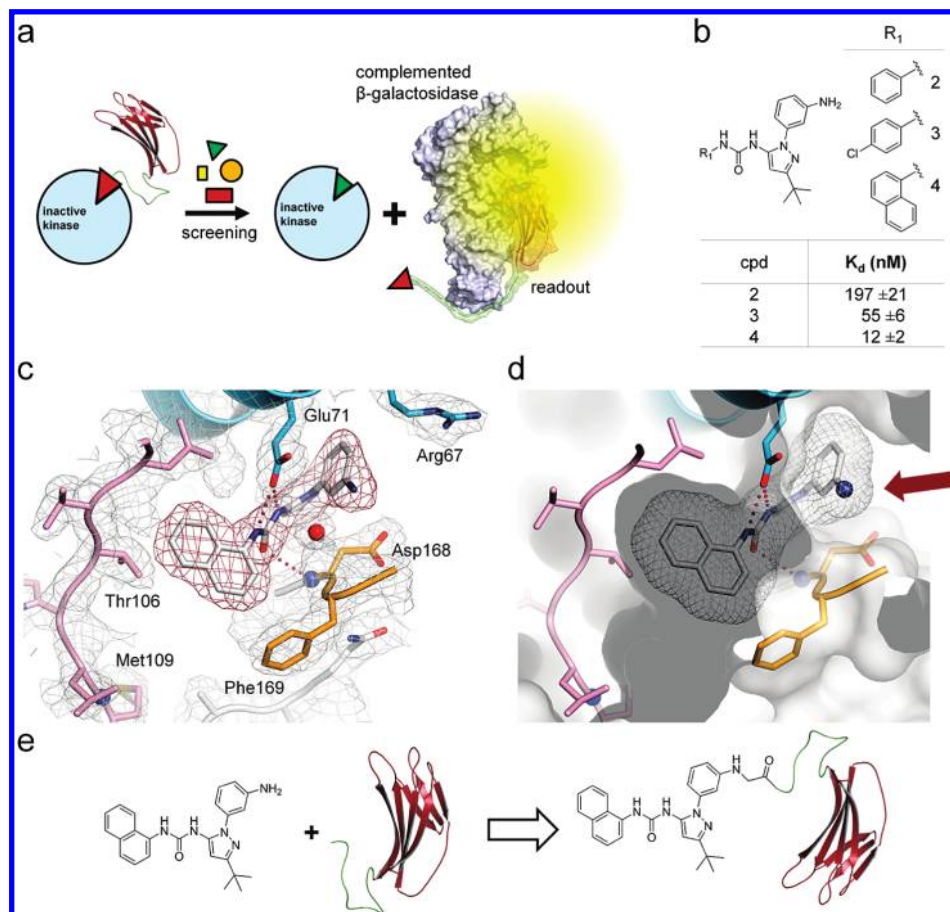
Figure 1. Assay design and development. (a) Schematic representation of the structure-based assay principle (PDB code 1DPO).[44] The enzyme donor (ED)-ligand is bound to the allosteric site of the inactive kinase (DFG-out conformation). In a screening scenario, small molecules compete with the ED-ligand for binding to the kinase. The peptide portion of the displaced ED-ligand binds to a truncated form of β-galactosidase which is only active when complemented by the ED-ligand. The enzymatic activity of β-galactosidase is measured via luminescence as a result of ED-ligand displacement. (b) Evaluation of pyrazoloureas as potential allosteric probes for p38α. K_d values were obtained using a direct binding assay described previously.[23,24] Because of its high affinity to p38α, **4** was selected to serve as the inhibitor part of the ED-ligand. (c) Crystal structure of p38α in complex with **4**. The inhibitor is bound to the allosteric site of inactive p38α. The $2F_o - F_c$ electron density maps of the ligand (red) and the protein (gray) are contoured at 1σ. Hydrogen bonding interactions of the inhibitor with helix C (blue) and the DFG-motif (orange) are shown as red dotted lines. (d) Surface representation of the allosteric binding site of p38α (gray) with bound ligand (gray mesh) revealing the correct positioning of the amino group (blue sphere) to serve as an anchor point for further attachment of the β-galactosidase peptide (red arrow). (e) Chemical structure of compound **4** and schematic representation of the ED-ligand probe. For assay validation two molecules of compound **4** were linked to the ED peptide (see Schemes 1 and 2).

Scheme 1. Acetylation, Hydrolysis, and Maleimide Linker Synthesis of 4 (Type III Inhibitor)
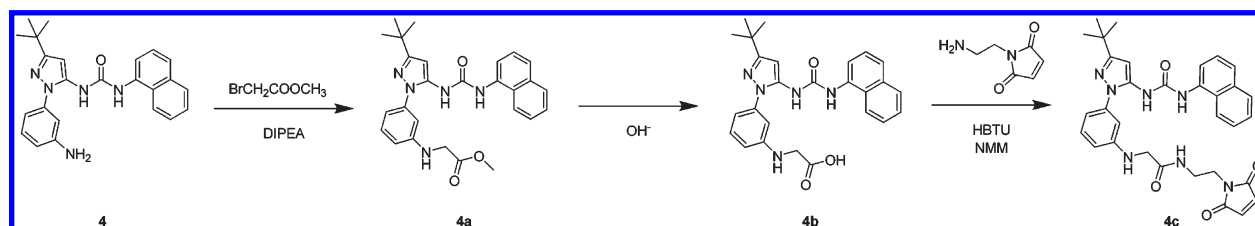
chemiluminescent read-out signal. In the absence of displacing ligands, it does not allow EFC with β-galactosidase to occur, thereby resulting in minimum background signal. Competitive displacement of the ED conjugate from the kinase occurs in the presence of compounds which bind to the allosteric site, allowing it to freely complement the EA and generate a chemiluminescence signal as the assay readout.[15,16] The ligand portion of the ED probe, which has the ability to bind within the allosteric pocket of the kinase, was first crystallized with the target. The protein X-ray structure was solved in order to verify

that the ED peptide conjugate binds to the inactive state of the kinase without causing any unexpected steric clashes (Figure 1c,d). The crystal structure revealed the ideal point of attachment for the conjugation of the β-galactosidase ED peptide fragment to the ligand. This ED conjugate was then validated against p38α kinase using a series of known inhibitors in conjunction with additional SAR studies and validation of ligand binding modes by protein X-ray crystallography. To get an idea about the applicability of this system to other kinases, the type III ligand portion of the ED probe was

Scheme 2. Chemical Conjugation of ED Peptide with Type III Inhibitor
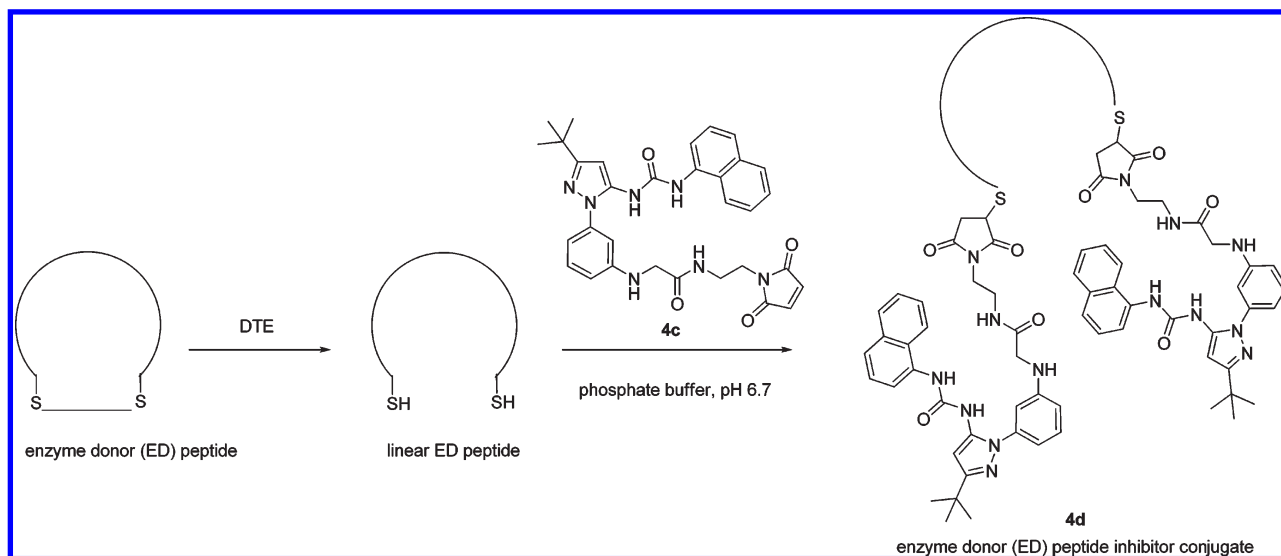
profiled against 58 kinases in a direct binding assay.[17,18] The results of this screen allowed the assay system to be extended to additional kinases for screening of inhibitors that stabilize inactive kinase conformations. Assay performance using enzymatically active and inactive p38α (phosphorylated and unphosphorylated) and the effect of added glycerol and DMSO were examined.

Results

Design of the Type III Inhibitor Probe for ED Conjugation. On the basis of the wealth of structural information available for several potent types II and III inhibitors in complex with p38α in the DFG-out conformation,[19−22] we chose the weak binder **1**, which was the lead compound used to develop the potent inhibitor **11** (BIRB-796),[19] as a model to design and synthesize three potent DFG-out inhibitors (**2**, **3**, **4**) (Figure 1b) carrying a meta aniline at the N1 position of the pyrazole moiety. On the basis of modeling studies, we predicted that this amine would point toward the solvent and would serve as a good anchor point for conjugation to the ED peptide without compromising the binding affinity of the molecule. To identify the best binder to use as a probe, we made use of a novel fluorescent-labeled kinase binding assay (FLiK) to directly determine the K_d of these allosteric ligands.[23] This assay confirmed that the measured compounds bind to and stabilize the inactive conformation of the kinase. We found that the naphthyl derivative **4** has the highest affinity for p38α kinase with a K_d of ~12 nM (Figure 1b).

Crystal Structure of a Type III Inhibitor with p38α. To verify that **4** adopts the proposed binding mode in the allosteric pocket with the newly introduced amino group pointing out of the binding site, we solved the crystal structure of this compound in complex with p38α (Figure 1c) (Table 1). **4** binds to the DFG-out conformation and resides in the allosteric site, as previously seen in the complex of the same compound with cSrc (PDB code 3F3T).[24] As expected from our modeling studies with p38α, the free anilino moiety points into the solvent and qualifies as an anchor point for further conjugation/modifications (Figure 1d). Thus, we chose this inhibitor to conjugate to the enzyme donor (ED) peptide and used this as the

probe to screen kinase inhibitors employing EFC technology (Figure 1e). **4** was conjugated to the ED peptide by a linker to yield the EFC probe, or ED-ligand, **4d** (Schemes 1 and 2). This ED-type III inhibitor conjugate was subsequently used for the validation of the assay.

Validation of the Enzyme Fragment Complementation (EFC) Assay System. Before using this system for IC$_{50}$ determination of competing ligands, we set up and validated the assay to ensure reliability and reproducibility. In general, the assay requires two steps: (i) an incubation step in which the target kinase, ED probe, and inhibitor are preincubated and (ii) a detection step in which the enzyme acceptor (EA) portion of β-galactosidase and its substrate are added to the mixture such that the generated chemiluminescence signal can be measured with time. The reproducibility and robustness of the assay, measured as the output of the reaction step, require that the kinase and ED-ligand have reached binding equilibrium during the incubation step. Furthermore, we titrated different concentrations of active p38α (activated via phosphorylation by the upstream kinase MKK6) and inactive p38α kinase (unphosphorylated) against the ED-ligand and verified that the luminescence signal is proportional to the ED-ligand−kinase complex (Figure 2a). Therefore, the luminescence signal observed in a screening scenario would be proportional only to the amount of ED-ligand displaced by an added inhibitor. We found that 12.5 and 75 nM of inactive and active p38α, respectively, are the highest concentrations of kinase that can be used to stay within the linear range of the luminescence signal. These concentrations were used for IC$_{50}$ determinations, since they yielded the largest dynamic range in signal change. The differences between these concentrations could result from the fact that inactive p38α is more likely to be in the DFG-out conformation, which is preferred by the ED-ligand, thus requiring 6-fold less kinase to scavenge up the ED-ligand. In the case of the active kinase, a conformational change in the activation loop must first occur to achieve the DFG-out conformation prior to binding of the ED-ligand. This preference for the inactive kinase was confirmed by measuring the binding constant (K_d) of the ED-ligand toward both active and inactive p38α (inactive p38α K_d = 3 ± 0.75 nM; active p38α K_d = 72 ± 20 nM). The fact that type III inhibitors show different
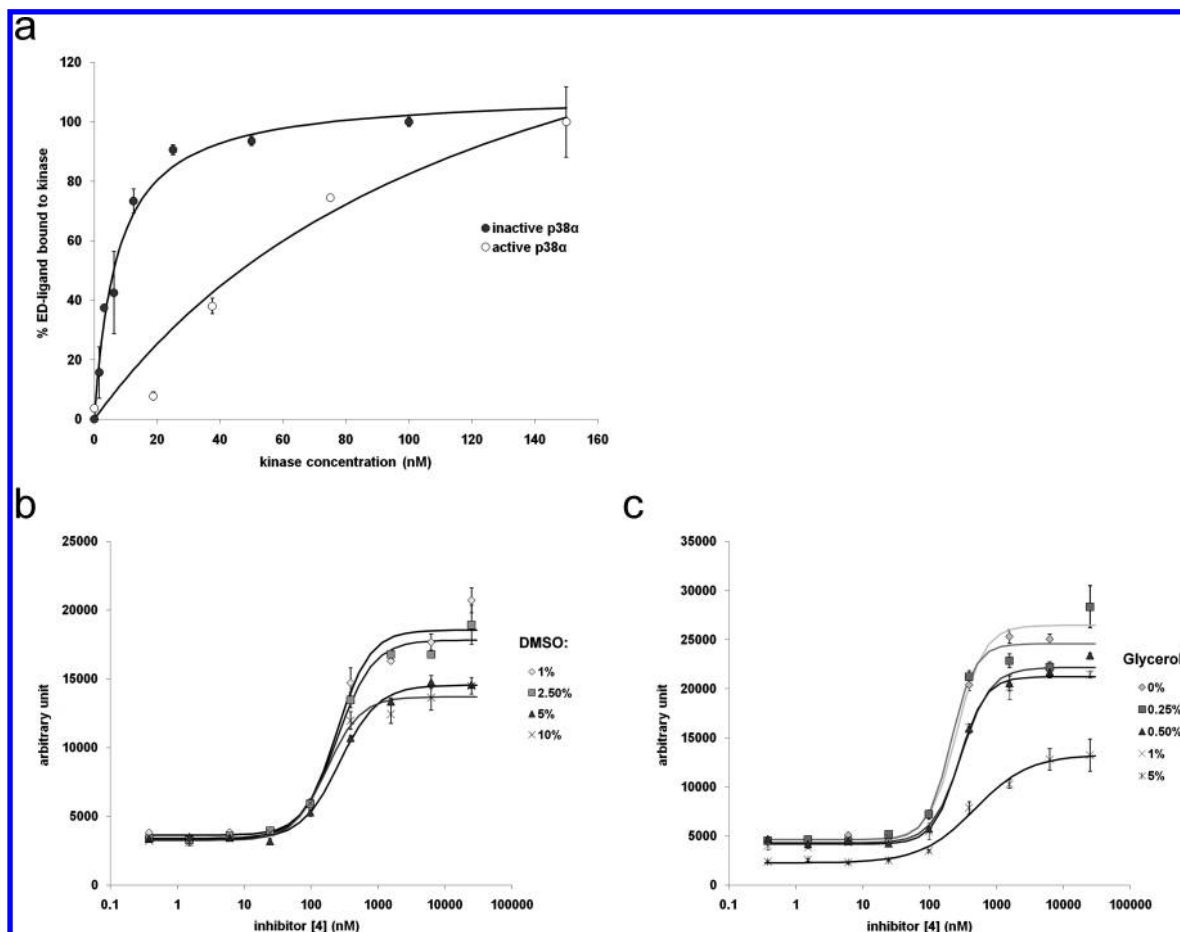
Figure 2. Validation of the assay system in p38α. (a) Increasing amounts of active (white circles) and inactive (black circles) kinase were titrated against 1.25 nM ED-ligand. The percentage of ED-ligand bound was calculated from the β-galactosidase signal representing the amount of free ligand in solution. (b, c) Dose response curves of **4** in the presence of DMSO and glycerol, respectively.

affinities to active and inactive kinases has been reported previously.[25,26] With the focus on stabilizers of the inactive conformation, inactive kinase was then used for further optimization and IC$_{50}$ determination. We also validated the additive tolerance of the assay by measuring the effect of DMSO and glycerol concentration. As shown in Figure 2b, a maximum of 2.5% DMSO (v/v) could be used in the assay, since higher amounts tend to lower the dynamic range (i.e., signal/noise ratio). A plausible explanation for the drop in the assay window with higher concentrations of DMSO could be the compromised stability of the kinase during prolonged incubation times. Similarly, glycerol at concentrations >1% (v/v) significantly lowers the dynamic range of the assay system (Figure 2c). To maintain the robustness of the assay, it is therefore important to minimize the amount of glycerol (a component found in many kinase storage buffers) in the final mixture. To attain equilibrium of the ED probe with the kinase, we titrated the ED-ligand against the enzyme acceptor (EA) to further optimize the assay response and to minimize background signal. We found that the amount of EA had little influence on the signal-to-noise ratio. With respect to different ED-ligand concentrations, the maximal signal-to-noise ratio was obtained using 4 nM ED-ligand together with equal amounts of the EA portion of β-galactosidase and chemiluminescence substrate solution. However, in order to increase the likelihood that the competing inhibitor added to the reaction mixture would successfully compete out the ED-ligand from

the target kinase, we chose only 1.25 nM ED-ligand at a small expense to the dynamic range (i.e., maximal signal is reduced when less ED-ligand is used). Having established the ideal concentrations of the various assay components, we set out to determine the shortest incubation and detection times needed to yield the highest signal. We found that the incubation time for the kinase and the ED-ligand had little effect on the signal-to-noise ratio of the readout and used a 2 h incubation time for further experiments. Although the detection step itself was shown to run linearly for at least 6 h, we chose a detection time of 1 h for convenience.

Characterization of Kinase Inhibitors. After optimizing the assay conditions, we turned our attention to the measurement of ED-ligand displacement by some known kinase inhibitors in order to further validate the assay response. Titration with unlabeled **4** yielded a sigmoidal dose response curve with IC$_{50}$ values in the nanomolar range (Figure 2b,c). This indicated that the ED conjugate can get displaced by suitable inhibitors and that the binding of ED probe to this site is specific and the ED probe can be used to identify and characterize small molecular binders of kinases. More importantly, the IC$_{50}$ value is consistent with the results obtained using an activity-based HTRF (homogeneous time-resolved fluorescence) kinase assay. Since there did not appear to be any dependence of the IC$_{50}$ on the pre-incubation (reaction) step, we used a 2 h incubation as standard for measuring the IC$_{50}$ of further compounds.

Table 1. Data Collection and Refinement Statistics for p38α with **4**, **12**, **19**, **21**, and **22**

	p38α with **4** (3HV7)	p38α with **12** (3HV6)	p38α with **19** (3HV3)	p38α with **21** (3HV4)	p38α with **22** (3HV5)
space group	$P2_12_12_1$	$P2_12_12_1$	$P2_12_12_1$	$P2_1$	$P2_1$
cell dimensions					
a, b, c (Å)	66.71, 74.52, 78.91	66.41, 74.66, 78.35	66.51, 74.52, 76.98	70.64, 74.06, 72.00	70.77, 74.12, 71.60
α, β, γ (deg)	90.00, 90.00, 90.00	90.00, 90.00, 90.00	90.00, 90.00, 90.00	90.00, 93.90, 90.00	90.00, 93.72, 90.00
resolution (Å)	40.0−2.40	40.0−1.95	40.0−2.00	40.0−2.60	40.0−2.25
	$(2.50-2.40)^a$	$(2.05-1.95)^a$	$(2.10-2.00)^a$	$(2.70-2.60)^a$	$(2.35-2.25)^a$
R_{sym} or R_{merge} (%)	6.9 (35.7)	3.3 (21.7)	4.3 (37.5)	11.1 (49.9)	4.6 (25.0)
$I/\sigma I$	17.7 (5.2)	19.1 (7.7)	19.8 (4.9)	19.1 (5.4)	19.8 (4.5)
completeness (%)	99.9 (100)	99.7 (99.9)	98.8 (98.8)	99.5 (99.3)	99.0 (99.3)
redundancy	4.8 (4.8)	4.7 (4.6)	4.8 (4.9)	3.5 (3.5)	2.6 (2.6)
refinement					
resolution (Å)	40.0−2.40	40.0−1.95	40.0−2.00	40.0−2.60	40.0−2.25
no. reflections	15869	28963	26160	22868	34893
R_{work}/R_{free}	20.3/27.9	20.9/25.4	23.0/30.0	19.4/27.1	18.8/26.0
no. atoms					
protein	2661	2668	2718	5434	5453
ligand/ion	50	70	64	148	152
water	107	177	124	157	295
B-factors	27.0	29.9	41.0	17.6	28.2
protein	27.2	29.6	40.9	17.5	28.2
ligand/ion	17.6	33.4	41.3	23.3	29.0
water	25.7	33.2	43.0	13.7	27.0
rms deviations					
bond lengths (Å)	0.016	0.015	0.016	0.014	0.016
bond angles (deg)	1.620	1.503	1.542	1.598	1.613
wavelength (Å)	1.54170	1.54170	1.00000	0.97703	1.54170
temperature (K)	100	100	90	90	100
X-ray source	Bruker AXS Microstar	Bruker AXS Microstar	SLS	SLS	Bruker AXS Microstar
Ramachandran plot					
residues in					
most favored regions (%)	87.8	90.2	89.0	85.9	89.0
additional allowed regions (%)	11.2	9.5	10.3	13.5	10.8
generously allowed regions (%)	1.0	0.3	0.7	0.7	0.2
disallowed regions (%)	0.0	0.0	0.0	0.0	0.0

^{a} For all p38α complex structures, diffraction data from one crystal were used to determine the structure. Values in parentheses are for the highest resolution shell.

Using these optimized conditions, we determined IC$_{50}$ values for a set of 30 compounds chosen to represent the three kinase inhibitor types known for p38α (Chart 1, Table 2). Staurosporine (**30**),[18] which is a nonbinder of p38α, served as a negative control and as expected did not displace the ED-ligand. **10** was also used as a negative control because its 2,6-dicloro-3-trifluormethylphenyl moiety does not fit into the allosteric pocket because of steric hindrance.[23] No interference of β-galactosidase enzyme activity was detected for any of the compounds tested in the EFC kinase binding assay (data not shown). We observed mean Z'-factors of 0.7−0.8. The Z'-factor is a measure of the statistical quality or power of a high-throughput screening (HTS) assay,[27] and the Z'-factors generated by the EFC assay are more than suitable for screening large compound libraries.

X-ray Crystallographic Analysis. To better understand the affinity profiles of all tested compounds, we solved the crystal structures of quinolines **19**, **21**, and **22** as well as of **12**, an analogue of **11**, in complex with p38α (Figure 3) (Table 2). **12** was chosen to help explain its 10-fold lower binding potency when compared to **11**, a closely related derivative and a well-known type II p38α inhibitor[20] (Figure 3). Regan and co-workers recently reported a lower potency of **12** when compared to **11** and argued that the loss of hydrophobic interactions observed when the naphthyl moiety of **11** interacts with the lipophilic subpocket behind the gatekeeper residue Thr106 could result in an unfavorable orientation of the ethoxymorpholino unit of **12**, preventing an effective hinge region contact.[22] However, superimposition of p38α−**12** with the p38α−**11** complex (PDB code 1KV2) revealed that both ligands align almost perfectly, adopting the same binding site geometries including a hydrogen bond to the backbone of Met109 of the hinge region (Figure 3a). Therefore, the significant increase in binding affinity observed for **11** is solely due to its naphthyl moiety which, compared to the phenyl ring of **12**, limits conformational flexibility and penetrates much deeper into the hydrophobic backpocket, thereby substantially increasing binding affinities to p38α. This further highlights the importance of this subpocket for ligand binding in p38α. We observed a similar trend when comparing the binding characteristics of the 1,4-fused quinoline **19** and the 1,3-fused quinoline **21**, respectively (Figure 3b). In both structures, the quinoline moiety of the ligand binds via a hydrogen bond to the hinge region and adopts a binding mode isostructural to quinazoline-based type II inhibitors of p38α.[13,23] However, the phenyl moiety that connects the hinge region binding portion of the ligands with the pyrazolourea portion clearly shows that the 1,3-fused molecule **21** accommodates the hydrophobic pocket much better than the 1,4-fused compound **19** because of its more favorable binding geometry.

Chart 1. Type I, II, and III Inhibitors

Chart showing Scaffolds/Inhibitors (1-12, 13-16, 17-18, 19-20, 21-24, 25, 26 (SCIO-469)[41], 27 (AMG-548)[42], 28 (SKF-86002)[19], 29 (PP1)[43], 30) with Entry, R1, R2 columns for entries 1–24.

Table 2. IC$_{50}$ Values of Type I, Type II, and Type III Inhibitors (Chart 1) for p38α and JNK2[a]

cpd	p38α kinase: IC$_{50}$ (nM)		cpd	p38α kinase: IC$_{50}$ (nM)		cpd	JNK2 kinase: IC$_{50}$ (nM)	
	EFC	HTRF		EFC	HTRF		EFC	HTRF
1	16800 ± 7400	21000 ± 8000	**16**	1100 ± 370	1500 ± 650	**4**	70 ± 25	90 ± 35
2	440 ± 40	1100 ± 260	**17**	420 ± 200	320 ± 20	**8**	440 ± 110	1300 ± 470
3	1100 ± 60	2000 ± 900	**18**	370 ± 30	460 ± 320	**11**	27 ± 7	150 ± 60
4	170 ± 30	90 ± 40	**19**	470 ± 70	900 ± 420	**12**	1800 ± 540	12600 ± 4300
5	220 ± 40	100 ± 6	**20**	420 ± 130	2400 ± 60	**14**	770 ± 15	570 ± 350
6	220 ± 170	120 ± 20	**21**	310 ± 50	290 ± 80	**17**	1200 ± 70	150 ± 30
7	45 ± 25	150 ± 80	**22**	95 ± 25	150 ± 40	**18**	1900 ± 820	1400 ± 500
8	1300 ± 180	1200 ± 260	**23**	230 ± 30	290 ± 160	**19**	100 ± 15	380 ± 170
9	680 ± 60	1100 ± 360	**24**	250 ± 90	140 ± 30	**27**	220 ± 60	76 ± 25
10	nb	nb	**25**	400 ± 140	1100 ± 710			
11	220 ± 170	250 ± 30	**26**	96 ± 50	36 ± 7			
12	2300 ± 260	5500 ± 2800	**27**	75 ± 25	35 ± 8			
13	760 ± 450	1800 ± 1400	**28**	820 ± 150	110 ± 40			
14	1400 ± 530	800 ± 220	**29**	1000 ± 150	2800 ± 520			
15	1000 ± 580	6000 ± 1400	**30**	nb	nb			

[a] The structures of type I, type II, and type III inhibitors are shown in Chart 1. On the basis of their binding mode to the kinase domain of p38α, the individual inhibitors are classified as follows: **1–12**, type III; **13–25**, type II; **26–30**, type I. IC$_{50}$ values were obtained using the developed EFC displacement assay (enzymatically inactive p38α and JNK2 (unphosphorylated)). For comparison, IC$_{50}$ values were measured with an activity based phosphorylation assay (HTRF) (enzymatically active p38α and JNK2 (phosphorylated)). Both assay systems give comparable and consistent IC$_{50}$ values, demonstrating that the displacement assay can be used for inhibitor screening.

Occupation of this pocket appears to be an important feature of these hybrid compounds and explains the overall better binding potency of the 1,3-quinoline hybrids compared to their 1,4-substituted counterparts. The same trend is conserved among
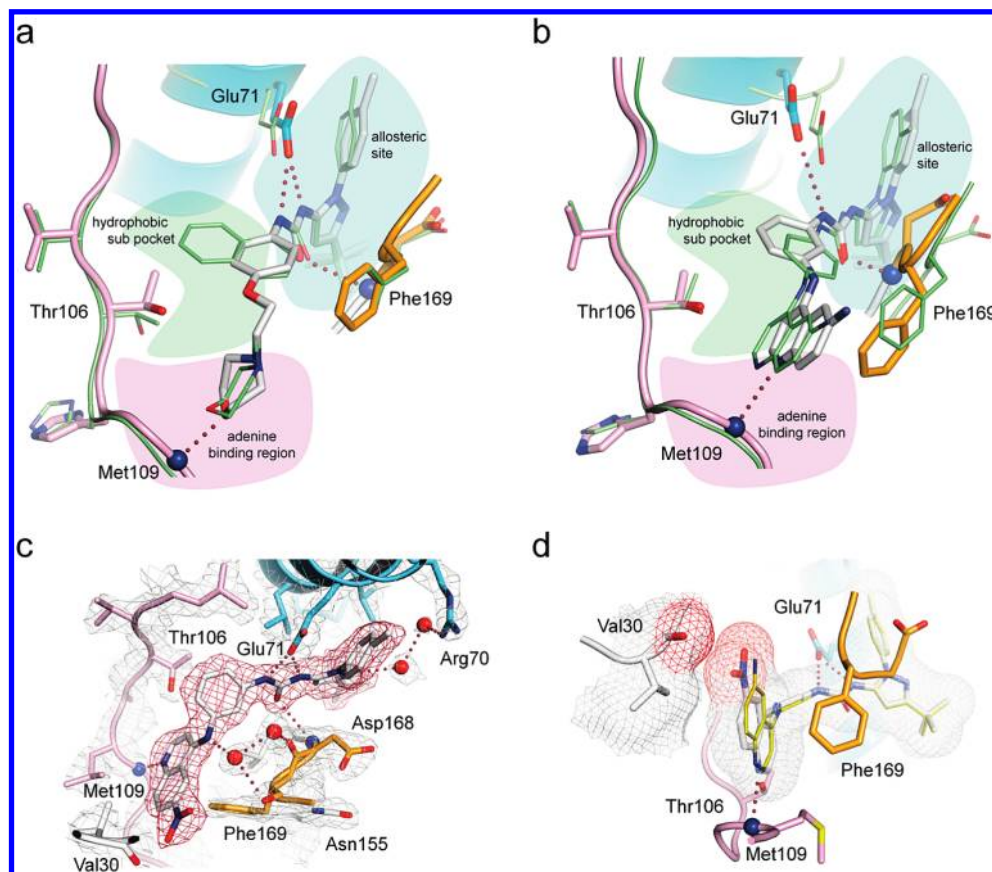
Figure 3. Crystal structures of various pyrazoloureas in complex with p38α. Colored areas in (a) and (b) represent different binding loci in and around the ATP cleft typically addressed by pyrazolourea-based type II inhibitors. The hinge region of the kinase is in pink. (a) Alignment of **12** (gray) with **11** (green) bound to p38α revealing the importance of the hydrophobic subpocket for ligand binding. (b) Overlay of the cocrystal structures of p38α with the 1,3-fused quinoline **21** (gray) and 1,4-fused quinoline **19** (green). **21** addresses the hydrophobic subpocket much better than **19**, resulting in a higher binding affinity. (c) Structure of the quinoline **22** bound to p38α. The $2F_o - F_c$ electron density maps of the ligand (red) and the protein (gray) are contoured at 1σ. (d) Overlay of **22** (gray) with the corresponding amine analogue **21** (yellow) in complex with p38α. Both molecules align well, and the quinoline cores form $\pi-\pi$ interactions with the side chain of Phe169 of the DFG-motif. The free amine of **21** and the nitro group of **22** in the 6-position of the quinoline core are in proximity to the backbone of Val30 of the glycine-rich loop.

quinazoline-based hybrid compounds as well (compare **14** and **16** to **17** and **18**).

Another interesting result of the structure−activity relationship studies (SAR) was the overall better binding potency of compounds that contain a nitro group in the 6-position of the quinazoline or quinoline inhibitor core when compared to their amino-substituted counterparts. To better understand this trend, we solved the crystal structure of the 6-nitro substituted quinoline **22** in complex with p38α and compared its binding mode with the amino substituted analogue **21** (Figure 3c,d). The ligand is well-defined by its electron density and adopts a binding mode typically observed for this class of type II inhibitors.[23] Superimposing both structures showed almost identical binding modes and gave no clear explanation for the increased binding affinity of **22** compared to **21** (Figure 3d). It is likely, however, that the different substituents in the 6-position of the quinazoline core (nitro versus amine) affect the strength of the $\pi-\pi$ interactions with the nearby side chain of Phe169 of the DFG motif and also influence the basicity of the quinoline nitrogen which forms the crucial hydrogen bond to the backbone of the hinge region. In summary, the presence of a nitro group on the quinoline core in combination with the 1,3 substitution pattern (deeper binding into the hydrophobic subpocket) may help to explain why **22** shows the highest affinity toward p38α of all tested hybrid compounds.

Selectivity, Profiling, and Extension of EFC Based Kinase Binding Assay to Additional Kinases. In order to determine selectivity profiles of the pyrazolourea **4** and to identify additional target kinases that (i) can adopt the DFG-out conformation and (ii) would be most likely suitable for the enzyme fragment complementation (EFC) assay, kinase inhibitor profiling was performed against a selected subpanel of 58 recombinantly expressed kinases[17] at 10 μM (Figure 4a). The inhibitor profile of **4** shows strong binding to surprisingly distinct kinases which most likely can adopt the DFG-out conformation. This finding can be explained on the basis of the comparison of crystal structures of **4** in complex with p38α and cSrc.[24] The naphthyl moiety of the ligand binds in a hydrophobic subpocket close to the gatekeeper residue. The differently sized gatekeeper side chains control access to the allosteric site from the direction of the hinge region and thereby serve as a critical determinant of inhibitor selectivity and affinity.[28,29] Facilitated by our ED-ligand probe, which is based on the type III binding mode **4**, we were able to adapt this assay format to additional kinases such as JNK2, DDR2, PDGFR-A, and RET (Figure 4b).

JNK2 Kinase Binding Assay. Out of the four additional kinases tested, we picked JNK2 for further validation and screened a selection of pyrazoloureas. Although the ED-ligand probe based on **4** has a lower affinity for JNK2, we were able to reliably study the SAR of several compounds
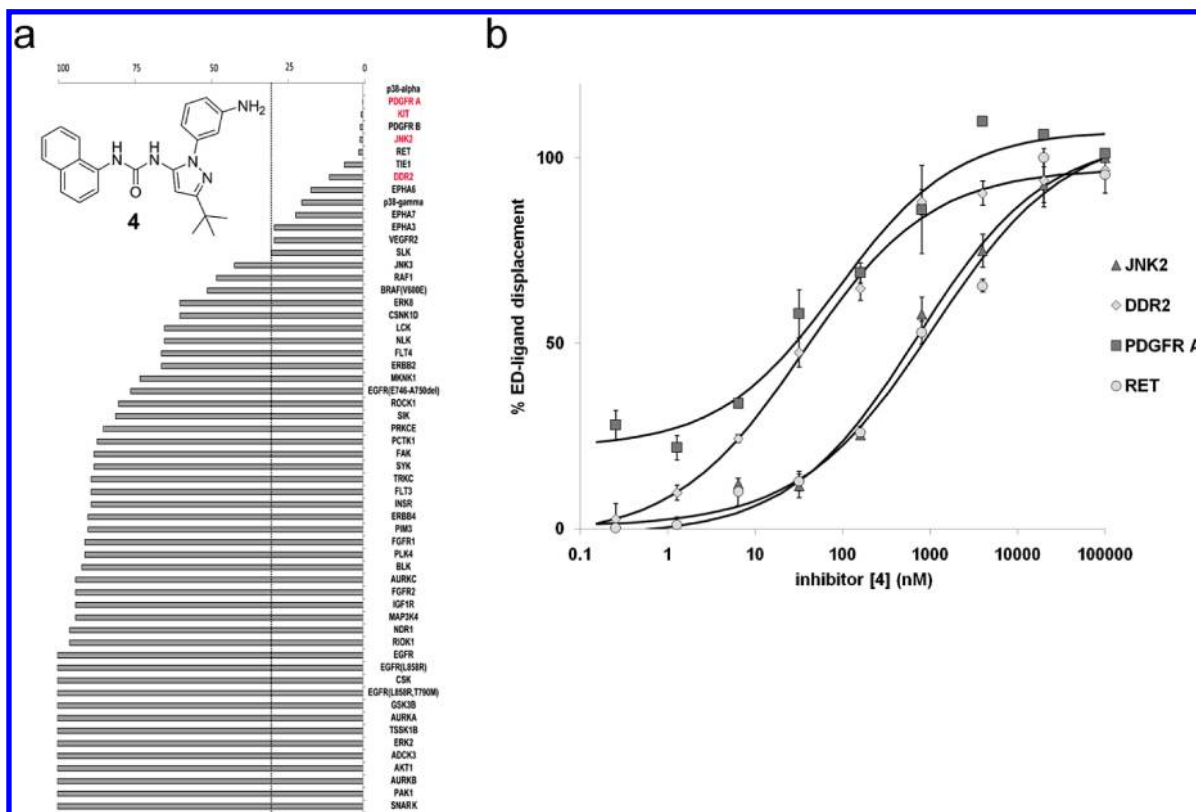
Figure 4. Kinase selectivity profile of a type III inhibitor and evaluation of the applicability of the EFC assay to other kinases. (a) Panel screen of the allosteric kinase inhibitor **4** at 10 μM against a subset of 58 human kinases employing the KINOMEscan binding assay (Ambit Biosciences). Weak or no binding is represented by a high number; tight binding is indicated by low numbers. A KINOMEscan score threshold of 30 (dashed lines) is used to dissect binders from nonbinders. (b) Dose response curves of **4** titrated against a panel of four kinases in the EFC assay demonstrate that the principle using an allosteric probe as a tool for drug discovery can be adapted to other kinases as well.

(Table 2). In contrast to what was observed in p38α, we found that the 1,4-fused hybrid compounds **14** and **19** are more potent when compared to their 1,3-fused counterparts **17** and **18**. In JNK2 kinase, access to the hydrophobic subpocket is regulated by a bulkier methionine (Met108)[30] gatekeeper while p38α carries a smaller amino acid (Thr106) at this position. In crystal structures of wild type cSrc and the drug resistant mutant variant cSrc-T338M in complex with **14**, we have recently observed that the central 1,4-fused phenyl moiety of the inhibitor avoids sterically demanding gatekeeper side chains via free rotation along the 1,4-axis.[13] Such observed flexibility likely explains the preference for these inhibitors with JNK2 kinase.

Discussion and Conclusion

Kinase inhibitor research has dramatically progressed in the past decade and has resulted in a variety of approved drugs for targeted therapies. However, several challenges such as the limited inhibitor selectivity of classical hinge region binders (type I) and acquired mutation-associated drug resistance remain to be solved. Ligands that address alternative binding pockets and thereby stabilize inactive kinase conformations are thought to offer new opportunities to circumvent these limitations. State of the art kinase assays rely on enzymatically active kinases and measure the perturbation of substrate phosphorylation as a means of target inhibition. Such formats require the kinase to be phosphorylated which shifts the equilibrium from the inactive DFG-out toward the enzymatically competent DFG-in conformation. As a direct consequence, binding of type II/III inhibitors to the DFG-out

conformation becomes more limited to detection and may result in an enrichment of hits of the type I scaffold in an HTS screening scenario. To address these needs, we developed and characterized a kinase binding assay based on enzyme fragment complementation technology which allows for the identification of small molecule stabilizers of inactive kinase conformations. To directly target a site outside the highly conserved ATP cleft, we used principles of structure-based ligand design to develop and synthesize type III inhibitors that would bind to the allosteric site of inactive (DFG-out) kinase conformations and allow for conjugation with an ED peptide fragment. The cocrystal structure of p38α in complex with compound **4** ultimately confirmed the precise binding mode and proved that the anilino moiety in the 3-position of the phenyl ring points out into the solvent and serves as a good anchor point for further attachments of the ED peptide using different linkers. We showed that displacement of the type III inhibitor−ED peptide conjugate by suitable binders leads to an increased signal, allowing a luminescence reaction to serve as the readout for the assay system. Facilitated by this assay system, we then determined IC$_{50}$ values for various type II and III ligands with high reproducibility and robustness. The setup of the assay is simple and straightforward and, most importantly, does not rely on enzymatically active kinase preparations, which is crucial for the enrichment of hits which bind to inactive kinase conformations. We feel that the detection system based on enzyme fragment complementation and chemiluminescence to identify stabilizers of the inactive kinase conformation offers major advantages over other fluorescence polarization-based approaches. We show

superior Z'-factors for our assay demonstrating its high sensitivity, which is often less optimal in fluorescence polarization experiments. The biggest advantage deals with the intrinsic fluorescence of inhibitors, which can be quite high in some small molecules, and often interferes with fluorescence-based approaches, thereby impairing the screening results and the detection of false hits. Lastly, we showed that the assay technique presented here can be applied to other kinases that can adopt the desired DFG-out conformation. Furthermore, the simple mix-and-ready approach of the assay, the miniaturization of the assay volume to 20 μL, and the good Z'-factors demonstrate that the kinase binding EFC assay can be employed to screen for type II and type III inhibitors as stabilizers of inactive kinase conformations in an HTS compatible format.

Experimental Section

Chemistry. Synthesis and characterization of compounds **1**−**24** have been described previously.[13,23,24] **25**−**29** were kindly provided by Merck-Serono (Darmstadt, Germany). **30** was purchased from Merck Chemicals (Darmstadt, Germany). All compounds have a purity of ≥95% as determined by HPLC coupled with mass spectrometry (HPLC−ESI-MS). HPLC−ESI-MS analyses were performed on an HPLC system from Agilent (1200 series) with an Eclipse XDB-C18 5 μm (column dimensions: 150 mm × 4.60 mm) column from Agilent and UV detection at 254 nm coupled to a Thermo Finnigan LCQ Advantage Max ESI spectrometer. Solvent system was H_2O with 0.1% formic acid (solvent A) and acetonitrile with 0.1% formic acid (solvent B) and was used at a flow of 1 mL/min. Gradient was a follows: 0 min, 90% solvent A/10% solvent B; 1 min, 90% solvent A/10% solvent B; 10 min, 0% solvent A/100% solvent B; 12 min, 0% solvent A/100% solvent B; 15 min, 90% solvent A/10% solvent B.

Synthesis of the Enzyme Donor (ED) Conjugate for Compound 4. The synthesis of the ED−inhibitor probe involves three steps (acetylation of **4** to **4a**, hydrolysis to **4b**, and maleimide linker coupling to **4c**) prior to ED conjugation to yield **4d**. Step by step procedures are outlined below.

Methyl 2-(3-(3-*tert*-Butyl-5-(3-naphthalen-1-ylureido)-1*H*-pyrazol-1-yl)phenylamino) acetate (4a). **4** (5 mg, 1.9 mmol) was suspended in 0.5 mL of anhydrous DMF followed by addition of diisopropylethylamine (2 equiv) and bromethyl acetate (1.1 equiv), and the mixture was stirred at ambient temperature for 4−5 h. The reaction was monitored on TLC and RP HPLC. The DMF was removed in vacuo, and the concentrated oil was subjected to purification by RP-HPLC (MeCN/H_2O with 0.1% TFA). The expected product was isolated and lyophilized to afford 3.7 mg (78%) of an amorphous powder. ESI-MS: [M + H^+] = 473 (found); 472 (calcd).

2-(3-(3-*tert*-Butyl-5-(3-naphthalen-1-ylureido)-1*H*-pyrazol-1-yl)phenylamino) acetic Acid (4b). A solution of **4a** (0.30 g, 1.78 mmol) was subjected to alkaline hydrolysis using MeOH−water and 2 N NaOH (100 μL) with the pH maintained at 9.0 at ambient temperature for 1 h. The reaction was monitored on RP HPLC. The solvent was concentrated under reduced pressure and the residue purified by RP HPLC (MeCN/H_2O with 0.1% TFA). The pure fraction was lyophilized to afford 1.8 mg (40%) of the pure product. ESI-MS: [M − H^+] = 456 (found); 457 (calcd).

2-(3-(3-*tert*-Butyl-5-(3-naphthalen-1-ylureido)-1*H*-pyrazol-1-yl)phenylamino)-*N*-(2-(2,5-dioxo-2,5-dihydro-1*H*-pyrrol-1-yl)ethyl)acetamide (4c). A solution of derivatized compound **4b** (1.5 mg, 0.68 mmol) was dissolved in 0.5 mL of anhydrous DMF and cooled at 0 °C followed by the addition of HBTU (1.2 mg, 0.45 mmol). *N*-(2-Aminoethyl)maleimide TFA (1.92 g, 0.3 mmol) freshly prepared in anhydrous DMF (100 μL) was neutralized with *N*-methylmorpholine (2 μL) and added to the above

solution. The reaction mixture was stirred at ambient temperature overnight. The solvent was concentrated under reduced pressure on a rotary evaporator and the residual oil subjected to purification using RP-HPLC to afford 1.0 mg of pure product. ESI-MS: [M+] = 580 (found); 580 (calcd).

Reduction of Linear Enzyme Donor (ED) Peptide. Enzyme donor (ED) peptide (5 mg) was dissolved in water (1 mL) and treated with DTE (5 mg) overnight at ambient conditions followed by RP-HPLC purification (MeCN/H_2O with 0.1% TFA) to yield pure 2.5 mg (50%) linear ED having free sulfhydrils. This was then immediately employed in the next step for conjugation with **4c**.

Conjugation of ED Peptide with Compound 4c (4d). To the above freshly purified linear ED (2.8 mL, 100 μM), 100 mM sodium phosphate buffer, pH 8.0 (200 μL), was added to adjust the pH to be between 6.3 and 6.7. To this, water (1 mL) and DMF (100 μL) were added, and 10-fold excess of maleimide linked compound **4c** in DMF/H_2O (100 μL) was added dropwise under vigorous stirring for 5 min. The mixture was left at ambient conditions for 90 min, and then an aliquot was taken to monitor the reaction mixture on RP-HPLC and to ensure complete reaction of the ED peptide sulfhydrils. The ED-ligand conjugate was purified to homogeneity by RP-HPLC, and the pure fractions collected were lyophilized and resuspended in MeCN/H_2O mixture. The concentration of the enzyme donor (ED) inhibitor peptide conjugate was assessed by UV−vis spectroscopy with an extinction coefficient calculated to be 36,300 at 280 nm (~15−20% unoptimized yield). MALDI-MS: [M^+] = 6549 (found); 6549 (calcd).

Materials. All reagents, fine chemicals, and solvents were purchased from Acros, Fluka, Sigma, Aldrich, or Merck, unless otherwise stated in the text. Crystallization plates (Easy Xtal Tool; 24-well) were obtained from Qiagen GmbH (Hilden, Germany). White microtiter plates in a 384-well small volume format used for EFC assay and HTRF assay were obtained from Greiner Bio-One GmbH (Solingen, Germany). Reagents for the activity-based assay were purchased from Cisbio (Bagnols-sur-Cèze, France). All kinases, except for p38α, were obtained from Invitrogen (Carlsbad, CA). For synthesis of the enzyme donor conjugate of **4**, RP HPLC was performed on a Waters 600 equipped with a PDA detector and a Zorbax 300A C18 semiprep column. Other reagents such as enzyme acceptor (EA) enzyme core assay buffer, chemiluminescent (CL) substrate, and enzyme donor dilution buffer (EDDB) were from DiscoveRx, Fremont, CA. The enzyme donor (ED) peptide was synthesized by American Peptide, Sunnyvale, CA.

Kinase Expression and Purification. The p38α construct was cloned into a pNFG vector and was transformed as an N-terminal His-tag construct with thrombin cleavage site into BL21(DE3) Rosetta *E. coli*. Cultures were grown at 37 °C until an OD_{600} of 0.5 was obtained, cooled to 18 °C using an ice bath, and then induced with 0.5 mM IPTG for overnight (~20 h) expression at 18 °C while shaking at 160 rpm. Cells were lysed in buffer A (50 mM Tris, pH 8.0, 500 mM NaCl + 5% glycerol + 25 mM imidazole) and loaded onto a 30 mL Ni column (self-packed), washed with 3 column volumes (CV) of Ni buffer A, and then eluted with a 0−50% linear gradient using Ni buffer B (Ni buffer A + 500 mM imidazole) over 2 CV. The protein was dialyzed for 5 h against dialysis buffer (25 mM HEPES, pH 7.0, 5% glycerol, 100 mM NaCl, 1 mM DTT) and then cleaved by incubating with thrombin protease (0.2 U/mg uncleaved protein) in a 50 mL falcon tube overnight at 4 °C. The protein was then centrifuged for 15 min at ~13 000 rpm to remove any precipitate that may have formed during the cleavage step. The supernatant was then taken and diluted at least 4-fold in anion buffer A (50 mM Tris, pH 7.4, 5% glycerol, 50 mM NaCl, 1 mM DTT) and loaded onto a 1 mL Sepharose Q FF column (GE Healthcare) and washed with 10 CV of anion buffer A. The protein was eluted with a 0−100% linear gradient of anion buffer B (anion buffer A + 600 mM NaCl) over 20 CV.

The protein was pooled and concentrated to 2 mL and passed through a Sephadex HiLoad 26/60 Superdex 75 column equilibrated with size exclusion buffer (20 mM HEPES, pH 7.1, 5% glycerol, 50 mM NaCl, 100 mg/L methionine, 10 mM DTT) at a rate of 2 mL/min. The eluted protein was then concentrated to ~15 mg/mL, aliquoted, and frozen at −80 °C.

Crystallization of p38α−Inhibitor Complexes. Various inhibitors were cocrystallized with purified p38α using conditions similar to those previously reported.[31] Briefly, protein−inhibitor complexes were prepared by mixing 40 μL of p38α (10−12 mg/mL) with 0.4 μL of inhibitor (100 mM in DMSO) and incubating the mixture for 1−2 h on ice. Crystals were grown in 24-well crystallization plates using the hanging drop vapor diffusion method and by mixing 1.5 μL of protein−inhibitor solution with 0.5 μL of reservoir (100 mM MES, pH 5.6−6.2, 20−30% PEG4000, and 50 mM *n*-octyl-β-glucopyranoside).

Structure Determination, Refinement, and Crystallographic Statistics. For crystals of p38α with inhibitors, 20% glycerol was added to the reservoir buffer as a cryoprotectant before freezing in liquid nitrogen. Diffraction data of the p38α−**19** and p38α−**21** complex crystals were collected at the PX10SA beamline of the Swiss Light Source (PSI, Villigen, Switzerland) using wavelengths close to 1 Å. Diffraction data of the p38α−**4**, p38α−**12**, and p38α−**22** complexes were collected in-house. All data sets were processed with XDS[32] and scaled using XSCALE.[32] All p38α−inhibitor complex structures were solved by molecular replacement with PHASER[33] using the published p38α structures (PDB code 1ZYJ)[34] or (PDB code 2EWA)[8] as templates. The molecules in the asymmetric unit were manually modified using the program COOT.[35] The model was first refined with CNS[36] using simulated annealing to reduce model bias. The final refinement was performed with REFMAC.[37] Inhibitor topology files where generated using the Dundee PRODRG2 server.[38] Refined structures were validated with PROCHECK.[39] Data collection, structure refinement statistics, PDB codes, and further details for the data collection as well as Ramachandran plot results are shown below in Table 2. PyMOL[40] was used to produce the figures.

Activation of p38α Kinase. Active MKK6 (T207E, T211E) (as purchased from Invitrogen) was diluted to 0.83 μg/mL together with inactive p38α (3.33 μg/mL final concentration) in buffer containing 50 mM Tris-HCl (pH 7.5), 1 mM Na_3VO_4, 0.01% NP-40, 0.1 mg/mL BSA, 2 mM DTT, 10 mM $MgCl_2$, 1 mM EGTA and was incubated together with 200 μM ATP at 30 °C for 1 h with constant agitation. ATP was subsequently removed by overnight dialysis in buffer containing 25 mM Tris, pH 8.0, 150 mM NaCl, and 10% (v/v) glycerol.

IC_{50} Determination with a Biochemical in Vitro HTRF Assay. IC_{50} determinations based on an enzyme activity assay were measured with the HTRF approach. GST-tagged ATF2 (200 nM) was obtained from CST (Boston, MA) and used as a substrate, and after 45 min of incubation time, 4 ng/μL of an antiphosphotyrosine antibody labeled with europium cryptate was added together with 12.5 nM of an anti-GST antibody labeled with the fluorophore D2. The FRET between europium cryptate and D2 was measured to quantify the phosphorylation of the ATF2. ATP and substrate concentrations were set at the K_M values, and kinases were used in concentrations of 1 ng/μL for activated p38α and 0.65 ng/μL for activated JNK2. A Safire^2 plate reader (Tecan) was used to measure the fluorescence of the samples at 620 nm (Eu-labeled antibody) and 665 nm (D2-labeled antibody) 60 μs after excitation at 317 nm. The quotient of both intensities for reactions made with nine different inhibitor concentrations was fit to a Hill four-parameter equation to determine IC_{50} values. Each reaction was performed in duplicate or triplicate on at least three independent occasions.

Optimization of the EFC Assay System and IC_{50} Determination. For the determination of a suitable kinase concentration, 5 μL of kinase at a given concentration was diluted in EFC buffer (35 mM HEPES, pH 7.4, 20 mM NaCl, 0.4 mM EGTA, 0.01% Tween-20, 10 mM $MgCl_2$, 0.1% bovine gamma globulins) and added to 5 μL of ED-ligand in a final concentration of 1.25 nM to initiate the kinase incubation reaction. After 2 h of incubation, 5 μL of enzyme acceptor (EA) and 5 μL of the chemiluminescence substrate (CL substrate) (both from DiscoveRx "Kinase Binding Assay Detection Kit") were included for the complementation reaction for 1 h or more before measuring the plate.

IC_{50} determinations of inhibitors were carried out by preparing nine 50-fold inhibitor dilutions prepared in DMSO and diluted in EFC assay buffer to have a 2% DMSO/buffer solution. Then 2.5 μL of 4× kinase (12.5 nM final concentration) and 2.5 μL of 4× ED-ligand (1.25 nM final concentration) were incubated together with 5 μL of inhibitor/buffer solution for 2 h prior to a 1 h complementation reaction. The final DMSO concentration was 1%, and inhibitor concentrations ranged from 100 μM to 1.5 nM. Chemiluminescence was measured with a Tecan Safire^2 plate reader.

Dose Response Curve of Compound 4 on PDGFR B, DDR2, RET, and JNK2. The same protocol as described for IC_{50} determination in p38α kinase was used except the reaction time of β-galactosidase formation was only 10 min before measuring. Kinases were used at a concentration of 75 nM for PDGFR B (P3082, enzymatically active), DDR2 (PV3870, enzymatically active), and RET (PV3819, enzymatically active), while 150 nM was chosen for JNK2 (PV3621, enzymatically inactive).

References

(1) Sandoval, D. A.; Obici, S.; Seeley, R. J. Targeting the CNS to treat type 2 diabetes. *Nat. Rev. Drug Discovery* **2009**, *8*, 386–398.

(2) Cohen, P. Targeting protein kinases for the development of anti-inflammatory drugs. *Curr. Opin. Cell Biol.* **2009**, *21*, 317–24.

(3) Fabbro, D.; Ruetz, S.; Buchdunger, E.; Cowan-Jacob, S. W.; Fendrich, G.; Liebetanz, J.; Mestan, J.; O'Reilly, T.; Traxler, P.; Chaudhuri, B.; Fretz, H.; Zimmermann, J.; Meyer, T.; Caravatti, G.; Furet, P.; Manley, P. W. Protein kinases as targets for anticancer agents: from inhibitors to useful drugs. *Pharmacol. Ther.* **2002**, *93*, 79–98.

(4) Gaestel, M.; Kotlyarov, A.; Kracht, M. Targeting innate immunity protein kinase signalling in inflammation. *Nat. Rev. Drug Discovery* **2009**, *8*, 480–499.

(5) Zhang, J.; Yang, P. L.; Gray, N. S. Targeting cancer with small molecule kinase inhibitors. *Nat. Rev. Cancer* **2009**, *9*, 28–39.

(6) Janne, P. A.; Gray, N.; Settleman, J. Factors underlying sensitivity of cancers to small-molecule kinase inhibitors. *Nat. Rev. Drug Discovery* **2009**, *8*, 709–723.

(7) Bogoyevitch, M. A.; Fairlie, D. P. A new paradigm for protein kinase inhibition: blocking phosphorylation without directly targeting ATP binding. *Drug Discovery Today* **2007**, *12*, 622–633.

(8) Vogtherr, M.; Saxena, K.; Hoelder, S.; Grimme, S.; Betz, M.; Schieborr, U.; Pescatore, B.; Robin, M.; Delarbre, L.; Langer, T.; Wendt, K. U.; Schwalbe, H. NMR characterization of kinase p38 dynamics in free and ligand-bound forms. *Angew. Chem., Int. Ed.* **2006**, *45*, 993–997.

(9) Backes, A. C.; Zech, B.; Felber, B.; Klebl, B.; Müller, G. Small-molecule inhibitors binding to protein kinase. Part II: the novel pharmacophore approach of type II and type III inhibition. *Expert Opin. Drug Discovery* **2008**, *3*, 1427–1449.

(10) Liu, Y.; Gray, N. S. Rational design of inhibitors that bind to inactive kinase conformations. *Nat. Chem. Biol.* **2006**, *2*, 358–364.

(11) Ma, H.; Deacon, S.; Horiuchi, K. The challenge of selecting protein kinase assays for lead discovery optimization. *Expert Opin. Drug Discovery* **2008**, *3*, 607–621.

(12) Olive, D. M. Quantitative methods for the analysis of protein phosphorylation in drug development. *Expert Rev. Proteomics* **2004**, *1*, 327–341.

(13) Getlik, M.; Grütter, C.; Simard, J. R.; Klüter, S.; Rabiller, M.; Rode, H. B.; Robubi, A.; Rauh, D. Hybrid compound design to overcome the gatekeeper T338M mutation in cSrc. *J. Med. Chem.* **2009**, 3915–3926.

(14) Naqvi, T.; Rouhani, R.; Singh, R. Improved Receptor Detection. WO 2003102154 (A2), **2003**.

(15) Zaman, G. J.; van der Lee, M. M.; Kok, J. J.; Nelissen, R. L.; Loomans, E. E. Enzyme fragment complementation binding assay for p38alpha mitogen-activated protein kinase to study the binding kinetics of enzyme inhibitors. *Assay Drug Dev. Technol.* **2006**, *4*, 411–420.

(16) Naqvi, T.; Rouhani, R.; Singh, R. Short Enzyme Fragment Donor. WO 03093786 (A2), **2006**.

(17) Fabian, M. A.; Biggs, W. H., 3rd; Treiber, D. K.; Atteridge, C. E.; Azimioara, M. D.; Benedetti, M. G.; Carter, T. A.; Ciceri, P.; Edeen, P. T.; Floyd, M.; Ford, J. M.; Galvin, M.; Gerlach, J. L.; Grotzfeld, R. M.; Herrgard, S.; Insko, D. E.; Insko, M. A.; Lai, A. G.; Lelias, J. M.; Mehta, S. A.; Milanov, Z. V.; Velasco, A. M.; Wodicka, L. M.; Patel, H. K.; Zarrinkar, P. P.; Lockhart, D. J. A small molecule−kinase interaction map for clinical kinase inhibitors. *Nat. Biotechnol.* **2005**, *23*, 329–336.

(18) Karaman, M. W.; Herrgard, S.; Treiber, D. K.; Gallant, P.; Atteridge, C. E.; Campbell, B. T.; Chan, K. W.; Ciceri, P.; Davis, M. I.; Edeen, P. T.; Faraoni, R.; Floyd, M.; Hunt, J. P.; Lockhart, D. J.; Milanov, Z. V.; Morrison, M. J.; Pallares, G.; Patel, H. K.; Pritchard, S.; Wodicka, L. M.; Zarrinkar, P. P. A quantitative analysis of kinase inhibitor selectivity. *Nat. Biotechnol.* **2008**, *26*, 127–132.

(19) Pargellis, C.; Tong, L.; Churchill, L.; Cirillo, P. F.; Gilmore, T.; Graham, A. G.; Grob, P. M.; Hickey, E. R.; Moss, N.; Pav, S.; Regan, J. Inhibition of p38 MAP kinase by utilizing a novel allosteric binding site. *Nat. Struct. Biol.* **2002**, *9*, 268–272.

(20) Cirillo, P. F.; Pargellis, C.; Regan, J. The non-diaryl heterocycle classes of p38 MAP kinase inhibitors. *Curr Top Med Chem* **2002**, *2*, 1021–1035.

(21) Sullivan, J. E.; Holdgate, G. A.; Campbell, D.; Timms, D.; Gerhardt, S.; Breed, J.; Breeze, A. L.; Bermingham, A.; Pauptit, R. A.; Norman, R. A.; Embrey, K. J.; Read, J.; VanScyoc, W. S.; Ward, W. H. Prevention of MKK6-dependent activation by binding to p38alpha MAP kinase. *Biochemistry* **2005**, *44*, 16475–16490.

(22) Regan, J.; Breitfelder, S.; Cirillo, P.; Gilmore, T.; Graham, A. G.; Hickey, E.; Klaus, B.; Madwed, J.; Moriak, M.; Moss, N.; Pargellis, C.; Pav, S.; Proto, A.; Swinamer, A.; Tong, L.; Torcellini, C. Pyrazole urea-based inhibitors of p38 MAP kinase: from lead compound to clinical candidate. *J. Med. Chem.* **2002**, *45*, 2994–3008.

(23) Simard, J. R.; Getlik, M.; Grütter, C.; Pawar, V.; Wulfert, S.; Rabiller, M.; Rauh, D. Development of a fluorescent-tagged kinase assay system for the detection and characterization of allosteric kinase inhibitors. *J. Am. Chem. Soc.* **2009**, *131*, 13286–13296.

(24) Simard, J. R.; Klüter, S.; Grütter, C.; Getlik, M.; Rabiller, M.; Rode, H. B.; Rauh, D. A new screening assay for allosteric inhibitors of cSrc. *Nat. Chem. Biol.* **2009**, *5*, 394–396.

(25) Frantz, B.; Klatt, T.; Pang, M.; Parsons, J.; Rolando, A.; Williams, H.; Tocci, M. J.; O'Keefe, S. J.; O'Neill, E. A. The activation state of p38 mitogen-activated protein kinase determines the efficiency of ATP competition for pyridinylimidazole inhibitor binding. *Biochemistry* **1998**, *37*, 13846–13853.

(26) Seeliger, M. A.; Nagar, B.; Frank, F.; Cao, X.; Henderson, M. N.; Kuriyan, J. c-Src binds to the cancer drug imatinib with an inactive Abl/c-Kit conformation and a distributed thermodynamic penalty. *Structure* **2007**, *15*, 299–311.

(27) Zhang, J. H.; Chung, T. D.; Oldenburg, K. R. A simple statistical parameter for use in evaluation and validation of high throughput screening assays. *J Biomol. Screening* **1999**, *4*, 67–73.

(28) Blencke, S.; Zech, B.; Engkvist, O.; Greff, Z.; Orfi, L.; Horvath, Z.; Keri, G.; Ullrich, A.; Daub, H. Characterization of a conserved structural determinant controlling protein kinase sensitivity to selective inhibitors. *Chem. Biol.* **2004**, *11*, 691–701.

(29) Daub, H.; Specht, K.; Ullrich, A. Strategies to overcome resistance to targeted protein kinase inhibitors. *Nat. Rev. Drug Discovery* **2004**, *3*, 1001–1010.

(30) Shaw, D.; Wang, S. M.; Villasenor, A. G.; Tsing, S.; Walter, D.; Browner, M. F.; Barnett, J.; Kuglstatter, A. The crystal structure of JNK2 reveals conformational flexibility in the MAP kinase insert and indicates its involvement in the regulation of catalytic activity. *J. Mol. Biol.* **2008**, *383*, 885–893.

(31) Bukhtiyarova, M.; Northrop, K.; Chai, X.; Casper, D.; Karpusas, M.; Springman, E. Improved expression, purification, and crystallization of p38alpha MAP kinase. *Protein Expression Purif.* **2004**, *37*, 154–161.

(32) Kabsch, W. Automatic processing of rotation diffraction data from crystals of initially unknown symmetry and cell constants. *J. Appl. Crystallogr.* **1993**, *26*, 795–800.

(33) Read, R. J. Pushing the boundaries of molecular replacement with maximum likelihood. *Acta Crystallogr., Sect. D: Biol. Crystallogr.* **2001**, *57*, 1373–1382.

(34) Michelotti, E. L.; Moffett, K. K.; Nguyen, D.; Kelly, M. J.; Shetty, R.; Chai, X.; Northrop, K.; Namboodiri, V.; Campbell, B.; Flynn, G. A.; Fujimoto, T.; Hollinger, F. P.; Bukhtiyarova, M.; Springman, E. B.; Karpusas, M. Two classes of p38alpha MAP kinase inhibitors having a common diphenylether core but exhibiting divergent binding modes. *Bioorg. Med. Chem. Lett.* **2005**, *15*, 5274–5279.

(35) Emsley, P.; Cowtan, K. Coot: model-building tools for molecular graphics. *Acta Crystallogr. D* **2004**, *60*, 2126–2132.

(36) Brünger, A. T.; Adams, P. D.; Clore, G. M.; DeLano, W. L.; Gros, P.; Grosse-Kunstleve, R. W.; Jiang, J. S.; Kuszewski, J.; Nilges, M.; Pannu, N. S.; Read, R. J.; Rice, L. M.; Simonson, T.; Warren, G. L. Crystallography & NMR system: a new software suite for macromolecular structure determination. *Acta Crystallogr., Sect. D: Biol. Crystallogr.* **1998**, *54*, 905–921.

(37) Murshudov, G. N.; Vagin, A. A.; Dodson, E. J. Refinement of macromolecular structures by the maximum-likelihood method. *Acta Crystallogr. D* **1997**, *53*, 240–255.

(38) Schüttelkopf, A. W.; van Aalten, D. M. PRODRG: a tool for high-throughput crystallography of protein−ligand complexes. *Acta Crystallogr., Sect. D: Biol. Crystallogr.* **2004**, *60*, 1355–1363.

(39) Laskowski, R. A.; McArthur, M. W.; Moss, D. S.; Thornton, J. M. PROCHECK: a program to check the stereochemical quality of protein structures. *J. Appl. Crystallogr.* **1993**, *26*, 263–291.

(40) DeLano, W. L. The PyMOL Molecular Graphics System. http://www.pymol.org, **2002**.

(41) Dominguez, C.; Powers, D. A.; Tamayo, N. p38 MAP kinase inhibitors: many are made, but few are chosen. *Curr. Opin. Drug Discovery Dev.* **2005**, *8*, 421–430.

(42) Lee, M. R.; Dominguez, C. MAP kinase p38 inhibitors: clinical results and an intimate look at their interactions with p38alpha protein. *Curr. Med. Chem.* **2005**, *12*, 2979–2994.

(43) Hanke, J. H.; Gardner, J. P.; Dow, R. L.; Changelian, P. S.; Brissette, W. H.; Weringer, E. J.; Pollok, B. A.; Connelly, P. A. Discovery of a novel, potent, and Src family-selective tyrosine kinase inhibitor. Study of Lck- and FynT-dependent T cell activation. *J. Biol. Chem.* **1996**, *271*, 695–701.

(44) Juers, D. H.; Jacobson, R. H.; Wigley, D.; Zhang, X. J.; Huber, R. E.; Tronrud, D. E.; Matthews, B. W. High resolution refinement of beta-galactosidase in a new crystal form reveals multiple metal-binding sites and provides a structural basis for alpha-complementation. *Protein Sci.* **2000**, *9*, 1685–1699.